PEIERLS STRUCTURAL TRANSITION IN ORGANIC CRYSTALS OF THE TTT_2I_3 TYPE IN A 2D APPROXIMATION

S. Andronic and A. Casian

Technical University of Moldova, Stefan cel Mare Avenue 168, Chisinau, MD-2004 Republic of Moldova
E-mail: andronic_silvia@yahoo.com

(Received May 29, 2019)

Abstract

The metal–insulator transition of the Peierls type is studied in organic crystals of tetrathiotetracene iodide with the lowest carrier concentration value in a 2D approximation. The two most important electron–phonon interaction mechanisms—of the deformation potential type and the polaron type—are considered. The dynamical interaction of carriers with defects is also taken into account. The renormalized phonon spectrum is calculated; it is shown that the transition is of the Peierls type.

1. Introduction

In the last years, quasi-one-dimensional (Q1D) organic crystals have attracted increasing attention in the scientific world due to more diverse and, in many cases, unusual properties exhibited by them. Organic nanomaterials have large potential applications in electronic, sensing, energy-harnessing, and quantum-scale systems [1]. It was also shown that highly conducting Q1D organic crystals can have extremely promising thermoelectric applications. Since not all parameters of these materials are well known, it is very important to apply different methods—both theoretical and experimental—to determine some of them. In this paper, we study the Peierls structural transition for this purpose.

This phenomenon was theoretically predicted by Rudolf Peierls. According to Peierls, at some lowered temperatures, a one-dimensional metallic crystal with a half filled conduction band has to pass in a dielectric state with a dimerized crystal lattice. This temperature is referred to as the Peierls critical temperature. The Peierls transition was studied by many authors [2–5]. To the best of our knowledge, the Peierls transition in tetrathiotetraceneiodide (TTT_2I_3) crystals has not been studied either theoretically, or experimentally. This material was synthesized independently and nearly simultaneously by the authors of [6–9] with the aim to find superconductivity in a low-dimensional conductor. At the same time, these crystals with the lowering temperature show a metal-dielectric transition. Earlier [10] we have shown for a crystal with a highest carrier concentration and the $TTT_2I_{3.1}$ composition that the transition is of the Peierls type.

For these crystals, the dimensionless Fermi momentum $k_F = 0.517\pi/2$. In this case, it was found that the Peierls transition begins at $T \sim 35$ K in TTT chains and considerably reduces the electrical conductivity. Due to interchain interaction, the transition is completed at $T \sim 19$ K.

The authors of [12] studied a 3D physical crystal model for the same curve. It was found that the transition begins at $T \sim 35$ K in TTT chains and is completed at $T \sim 9.8$ K, as observed

experimentally.

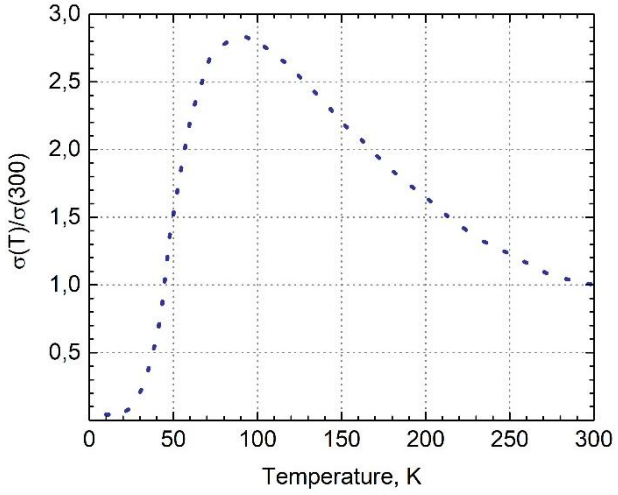

Fig. 1. Temperature dependence of electrical conductivity of the TTT2I3+δ crystal, δ = 0.01. Max – 90 K, σ → 0 at 20 K [10].

In this paper, we will study the behavior of the Peierls transition in TTT_2I_3 crystals with the lowest carrier concentration value. For simplicity, we will apply the 2D approximation. We will analyze the Peierls structural transition for the curve shown in Fig. 1. The dimensionless Fermi momentum in this case is k_F=0.502π/2. In addition, the Peierls critical temperature T_p is determined.

2. Physical Model of Crystals

The physical model of crystals was described in more detail in [11]. The Hamiltonian of the 2D crystal model in the tight binding and nearest neighbor approximations has the form

$$H = \sum_{\boldsymbol{k}} \varepsilon(\boldsymbol{k}) a_{\boldsymbol{k}}^{+} a_{\boldsymbol{k}} + \sum_{\boldsymbol{q}} \eta \omega_{\boldsymbol{q}} b_{\boldsymbol{q}}^{+} b_{\boldsymbol{q}} + \sum_{\boldsymbol{k},\boldsymbol{q}} A(\boldsymbol{k},\boldsymbol{q}) a_{\boldsymbol{k}}^{+} a_{\boldsymbol{k}+\boldsymbol{q}} (b_{\boldsymbol{q}} + b_{-\boldsymbol{q}}^{+}) \tag{1}$$

Here, the first term is the energy operator of free holes in the periodic field of the lattice. The hole energy is measured from the band top; it is presented in the following form:

$$\varepsilon(\boldsymbol{k}) = -2w_1(1-\cos k_x b) - 2w_2(1-\cos k_y a) \tag{2}$$

where w_1 and w_2 are the transfer energies of a hole from one molecule to another along the chain (x direction) and perpendicular to it (y direction).

In Eq. (1) $a_{\boldsymbol{k}}^{+}$, $a_{\boldsymbol{k}}$ are the creation and annihilation operators of the hole with a 2D quasi-wave vector $\boldsymbol{k}$ and projections (k_x, k_y); $b_{\boldsymbol{q}}^{+}$, $b_{\boldsymbol{q}}$ are creation and annihilation operators of an acoustic phonon with 2D wave vector $\boldsymbol{q}$ and frequency $\omega_{\boldsymbol{q}}$.

The second term in the Eq. (1) is the energy operator of longitudinal acoustic phonons

$$\omega_{\boldsymbol{q}}^2 = \omega_1^2 \sin^2(q_x b/2) + \omega_2^2 \sin^2(q_y a/2) \tag{3}$$

where ω_1 and ω_2 are the limit frequencies in the x and y directions.

The third term represents the electron–phonon interactions. The two most important electron–phonon interaction mechanisms—of the deformation potential type and the polaron type—are considered. The coupling constants of the first interaction are proportional to derivatives w_1' and w_2' of w_1 and w_2, with respect to the intermolecular distances. The coupling constant of second interaction is proportional to the average polarizability of the molecule α_0.

This interaction is important for crystals composed of large molecules, such as TTT, so that α_0 is roughly proportional to the molecule volume. The ratio of amplitudes of the polaron-type interaction to the deformation potential one in the *x* and *y* directions is described by parameters γ_1 and γ_2:

$$\gamma_1 = 2e^2\alpha_0 / b^5 w_1', \ \gamma_2 = 2e^2\alpha_0 / a^5 w_2' \tag{4}$$

The square module of matrix element $A(\boldsymbol{k},\boldsymbol{q})$ from Eq. (1) can be written in the form

$$\begin{aligned} |A(\boldsymbol{k},\boldsymbol{q})|^2 = 2\eta w_1'^2 /(NM\omega_{\boldsymbol{q}}) \times \{[\sin(k_x b) - \sin(k_x - q_x, b) - \gamma_1 \sin(q_x b)]^2 + \\ d_1^2[\sin(k_y a) - \sin(k_y - q_y, a) - \gamma_2 \sin(q_y a)]^2\}. \end{aligned} \tag{5}$$

Here, M is the mass of the molecule, N is the number of molecules in the basic region of the crystal, $d_1 = w_2/ w_1 = w_2' / w_1'$.

To explain the behavior of the electrical conductivity from Fig.1, it is necessary to take into account the dynamical interaction of carriers with defects. The static interaction will give contribution to the renormalization of the hole spectrum. Defects in TTT_2I_3 crystals are formed due to different coefficients of dilatation of TTT and iodine chains.

The Hamiltonian of this interaction H_{def} is presented as follows:

$$H_{def} = \sum_{\boldsymbol{k},\boldsymbol{q}} \sum_{n=1}^{N_d} B(q_x) \exp(-iq_x x_n) a_{\boldsymbol{k}}^{+} a_{\boldsymbol{k}-\boldsymbol{q}} (b_{\boldsymbol{q}} + b_{\boldsymbol{q}}^{-}) . \tag{6}$$

Here, $B(q_x)$ is the matrix element of a hole interaction with a defect; it is represented in the form

$$B(q_x) = \sqrt{\eta/(2NM\omega_q)} \cdot I(q_x), \tag{7}$$

where $I(q_X)$ is the Fourier transformation of the derivative with respect to intermolecular distance from the energy of interaction of a carrier with a defect and x_n numbers the defects that are considered linear along the *x*-direction of TTT chains and distributed randomly:

$$I(q_x) = D(\sin(bq_x))^2, \tag{8}$$

Where *D* is a parameter that determines the intensity of hole interaction with a defect. It has the same meaning as w_1' in (5) and is measured in $\text{eV}\cdot\text{Å}^{-1}$.

The renormalized phonon spectrum $\Omega(\boldsymbol{q})$ is determined by the pole of the Green function and obtained from the transcendent dispersion equation

$$\Omega(\boldsymbol{q}) = \omega_{\boldsymbol{q}}[1 - \overline{\Pi}(\boldsymbol{q},\Omega)]^{1/2}, \tag{9}$$

where the principal value of the dimensionless polarization operator takes the form:

$$\text{Re}\,\overline{\Pi}(\boldsymbol{q},\Omega) = -\frac{4}{\eta\omega_q} \sum_{\boldsymbol{k}} \frac{\left[|A(\boldsymbol{k},-\boldsymbol{q})|^2 + |B(q_x)|^2\right](n_k - n_{k+q})}{\varepsilon(\boldsymbol{k}) - \varepsilon(\boldsymbol{k}+\boldsymbol{q}) + \eta\Omega}. \tag{10}$$

Here, n_k is the Fermi distribution function. Equation (9) can be solved only numerically.

3. Results and Discussion

Numerical simulations for the 2D physical model of the crystal are performed for the following parameters [13]: $M = 6.5 \times 10^5 m_e$ (m_e is the mass of the free electron), $w_1 = 0.16$ eV, $w_1' = 0.26$ eV·Å^{-1}, $d_1 = 0.015$, $\gamma_1 = 1.7$, γ_2 is determined from the relationship: $\gamma_2 = \gamma_1 b^5 / a^5 d_1$, $k_F = 0.502\pi/2$. The sound velocity along TTT chains was estimated by comparison of the calculated results for the electrical conductivity of TTT_2I_3 crystals [13] with the reported ones [8], $v_{s1} = 1.5 \times 10^5$ cm/s. For v_{s2} in transversal direction (in a direction) we have taken 1.35×10^5 cm/s.

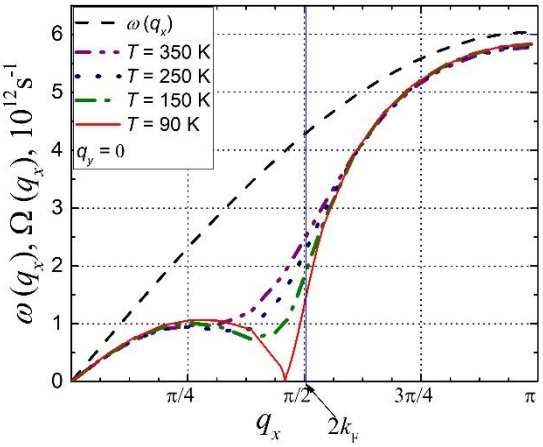

Fig. 2. Renormalized phonon spectrum $\Omega(q_x)$ for $\gamma_1 = 1.7$ and different temperatures. The dashed line is for the spectrum of free phonons. k_F=0.502 π/2, D = 1.074 eV·Å^{-1}.

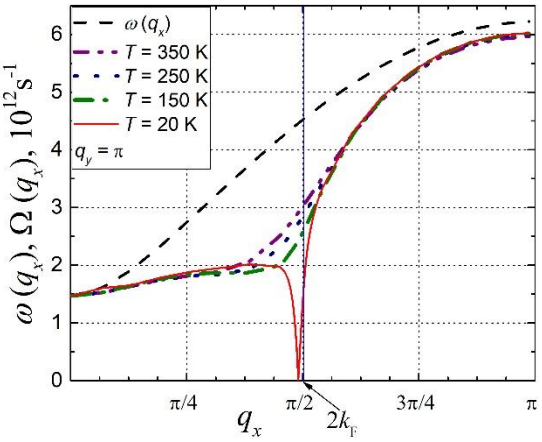

Fig. 3. Renormalized phonon spectrum $\Omega(q_x)$ for $\gamma_1 = 1.7$ and different temperatures. The dashed line is for the spectrum of free phonons. k_F=0.502π/2, D = 1.014 eV·Å^{-1}.

Figures 2 and 3 show the dependences of renormalized phonon frequencies $\Omega(q_x)$ as a function of q_x for different temperatures and different q_y values. In the same graphs, the dependences for initial phonon frequency $\omega(q_x)$ are shown. It is evident that the $\Omega(q_x)$ values are diminished in comparison with those of $\omega(q_x)$ in the absence of an electron–phonon interaction. This means that the electron–phonon interaction and structural defects diminish the values of lattice elastic constants. In addition, one can observe that, with a decrease in temperature T, the curves change their form, and a minimum appears in the $\Omega(q_x)$ dependences. This minimum becomes more pronounced at lower temperatures.

Figure 2 shows the case where $q_y = 0$ and dimensionless Fermi momentum $k_F = 0.502\pi/2$ and $D = 1.074$eV·Å^{-1}. Parameter D is a constant that determines the intensity of hole interaction with a defect. In this case, the interaction between TTT chains is neglected. The Peierls transition begins at $T = 90$ K. At this temperature, the electrical conductivity achieves a maximum. With the lowering temperature, the electrical conductivity decreases. Figure 3 shows the case where the interaction between TTT chains is taken into account ($q_y = \pi$), $D = 1.014$ eV·Å^{-1} and $k_F = 0.502\pi/2$. In this case, the transition is completed at $T = 20$ K. It was observed that parameter D decreases or the hole interaction with a defect is smaller in this case. It is evident from Fig. 1 that the electrical conductivity significantly decreases and achieves zero at $T \sim 20$ K.

4. Conclusions

The Peierls structural transition has been studied in existing organic crystals of TTT_2I_3 with the lowest hole concentration value. The 2D physical model has been considered. The two most important electron–phonon interaction mechanisms—of the deformation potential type and the polaron type—have been considered. The interaction of carriers with defects has been analyzed. The renormalized phonon spectrum has been calculated in the random phase approximation. The method of retarded temperature dependent Green function has been applied. It has been shown that the Peierls transition temperature strongly depends on iodine concentration. It has been found that, if $k_F = 0.502\pi/2$ and the hole concentration achieves the lowest value, the Peierls transition begins at $T \sim 90$ K in TTT chains and considerably reduces the electrical conductivity. Due to interchain interaction, the transition is completed at $T \sim 20$ K.

Acknowledgments

The authors express gratitude to the support of the scientific program of the Academy of Sciences of Moldova under project no. 15.817.02.22F.

References

[1] Organic Nanomaterials: Synthesis, Characterization, and Device Applications (edited by T. Torres and G. Bottari), John Wiley & Sons, Inc., Hoboken, NJ, USA, 2013.
[2] L. N. Bulaevskii, Usp. Fiz. Nauk 115, 263 (1975).
[3] M. Hohenadler, H. Fehske, and F.F. Assaad, Phys. Rev. B, 83, 115105 (2011).
[4] V. Solovyeva et al., J. Phys. D: Appl. Phys. 44, 385301 (2011).
[5] A. Chernenkaya, K. Medjanik, P. Nagel, M. Merz, S. Schuppler, E. Canadell, J. P. Pouget, and G. SchËonhense, Eur. Phys. J. B. 88, 13(2015).
[6] I.I. Buravov, G.I.Zvereva, V.F. Kaminskii, et al., Chem. Commun. 18, 720 (1976).
[7] V.F. Kaminskii, M.l. Kidekel', R.B. Lyubovskii, etal., Phys. Status Solidi A 44, 77 (1977).
[8] B. HiltiandC.W. Mayer, Helv. Chim. Acta 61, 501 (1978).
[9] L.G.Isset and E.A. Perz-Albuerene, Sol. State Comm., 21, 433 (1977).
[10] F. Shchegolev and E. B. Yagubskii, Extended Linear Chain Compounds (edited by I.S.Miller), Plenum Press, New York, 1982, vol. 2, p. 385.
[11] S. Andronic and A. Casian, Adv. Mater. Phys. Chem. 7,212 (2017).
[12] S. Andronic, I. Balmus, and A. Casian, 9th Int. Conf. on Microelectronics and Computer Science, Chisinau, Republic of Moldova, October, 19–21, 2017.
[13] A. Casian and I. Sanduleac, J. Electron. Mater. 43,3740 (2014).